This is a preprint, the final version is subject to change, of the American Mineralogist (MSA)
Cite as Authors (Year) Title. American Mineralogist, in press.
(DOI will not work until issue is live.) DOI: http://dx.doi.org/10.2138/am.2014.4792

Revision 1

Microporous gold:

Comparison of textures from Nature and experiments

Victor M. Okrugin[1,2], Elena Andreeva[1,2], Barbara Etschmann[3,4], Allan Pring[3], Kan Li[4], Jing Zhao[3,4], Grant Griffiths[5], Gregory R. Lumpkin[5], Gerry Triani[5] and Joël Brugger[3,*]

1. Institute of Volcanology and Seismology, Russian Academy of Science, Petropavlovsk-Kamchatsky, 683 006, Russia
2. Vitus Bering Kamchatka State University Petropavlovsk-Kamchatsky, 683 006 Russia
3. Mineralogy, South Australian Museum, North Terrace, Adelaide, 5000, South Australia
4. School of Chemical Engineering, The University of Adelaide, 5005, South Australia
5. Institute of Materials Engineering, Australian Nuclear Science & Technology Organisation, Kirrawee DC, NSW 2232, Australia

* Corresponding author: joel.brugger@adelaide.edu.au

Submitted to: American Mineralogist as a Letter

(max 15 pages of manuscript, one figure per page, separate title page).

Abstract

Recent experiments have shown that microporous gold can be obtained via the oxidative dealloying of Au(Ag)-tellurides such as calaverite ($AuTe_2$), krennerite (Au_3AgTe_8) and sylvanite ($(Au,Ag)_2Te_4$) under mild hydrothermal conditions. The same Au textures have been found in natural gold-telluride ores from the Late Miocene epithermal Aginskoe Au-Ag-Te deposit in Kamchatka, Russia. This confirms that natural microporous gold can form via the replacement of telluride minerals. This replacement may take place under hydrothermal conditions, e.g. during the late stage of the ore-depositing event, explaining the wide distribution of 'mustard gold' in some deposits. At Aginskoe, the oxidation of Au-tellurides appears to have resulted only in local redistribution of Au and Te, because the associated oxidation of chalcopyrite scavenged the excess Te, inhibiting the crystallization of secondary Te minerals more than a few μm in size. Such cryptic mobility may explain the lack of reported secondary Te minerals in many Te-bearing deposits.

Microporous gold in nature and aims of this study

Microporous gold, also known as 'mustard gold' (Wilson 1984), is a common product of the weathering of Au-Te ores (e.g., Ashanti Au deposit, Ghana, Bowell 1992; Kalgoorlie Au deposit, Western Australia, Wilson 1984). In some economic deposits, microporous gold can account for a large portion of the gold. For example, the Hercynian Dongping Au-Te Deposit (Hebei Province, People's Republic of China) contains in excess of 70 tons of Au (Nie, 1998), and Song et al. (1996) estimated that "secondary gold" accounts for 31-50% of gold at this deposit. Petersen et al. (1999) and Li and Makovicky (2001) showed that the microporous gold from Dongping results from the weathering of Au-(Ag) tellurides, in particular calaverite. In some grains, the porosity of the microporous gold from Dongping is open, but in others it is filled by a variety of oxide phases, including goethite, Pb-Te-oxides, Fe-Te-oxides, Te oxides, or Mn-Pb-(Te) oxides (Li and Makovicky, 2001).

The aims of this communication are to describe a new occurrence of microporous gold from the Aginskoe low sulfidation epithermal deposit in Central Kamchatka (Russia), and to compare the textures of microporous gold from this natural occurrence with those obtained experimentally via the dealloying of Au(Ag)-tellurides (calaverite, sylvanite and krennerite ;Zhao et al., 2009, 2010, 2013; Xu et al. 2013). We describe the different modes of Au, Te and Ag occurrence in the samples from Aginskoe, and for the first time we assess the role that hydrothermal fluids may play in the formation of microporous gold, as opposed to typical weathering processes.

Analytical methods and synthesis of microporous gold

The samples were imaged using a Quanta 450 FEG Environmental Secondary Electron Microscope (SEM) with Energy Dispersive Spectrometry (EDS) and a Silicon Drift Detector (SDD); sample compositions were measured using a CAMECA SX51 Electron Microprobe, operated at 15 keV and 20 nA. For most analyses, the beam was defocused to 5 μm diameter. Standards included Au (Au), Bi_2Se_3 (Se), PbS (Pb), Ag_2Te (Ag, Te), Sb_2S_3 (Sb) $CuFeS_2$ (Cu, Fe, S) and GaAs (As). Milling (Ga beam; 20-30 kV; currents ranging from 21 to 0.093 nA) and chemical X-ray mapping (20 kV) were done using a FEI Helios NanoLab Focused Ion Beam FIB–SEM (FEI, Netherlands).

We prepared microporous gold by dealloying both synthetic (pure $AuTe_2$; Sample 7-5) and natural calaverite (Sample 7-4; from the Golden Mile deposit in Kalgoorlie, Western Australia, South Australian Museum collection G29494; composition $Au_{0.94}Ag_{0.05}Sb_{0.02}Te_{2.00}$ according to Zhao et al. 2009). The synthetic calaverite was made following the procedure described by Deschênes et al. (2006).

These calaverite samples had grain sizes of <100 μm for synthetic and 75-150 μm for natural samples. They were heated at 200 °C in a Teflon-lined stainless steel cell using either (i) a buffer solution of 0.48 m $NaH_2PO_4 \bullet 2H_2O$ and 0.52 m H_3PO_4, resulting in a measured pH of 1.86 at 24.6 ˚C or (ii) a buffer solution of 0.66 m H_3BO_3 and 0.47 m NaOH, resulting in a measured pH of 9.83 at 21.3 ˚C. The reaction was conducted for 11 hours, after which the cells were removed from the oven and cooled to room temperature with the use of fans.

Modes of gold occurrence at the Aginskoe deposit

The Aginskoe deposit is a Late Miocene (6.9-7.1 My) Au-Ag deposit belonging to the Central Kamchatka epithermal district (Andreeva, et al. 2013; Takahashi et al. 2013). Samples 19 and 29 (A10) (South Australian Museum collection G33885 and G33896) were collected from the Aginskoe open pit, which has an elevation of 1230 m and is the most intensively oxidized part of the ore body. The ore consists of quartz and adularia ($KAlSi_3O_8$), displaying complex banding and brecciation (Andreeva et al. 2013). Ore minerals (mainly chalcopyrite) line some of the growth bands and some of the quartz clasts. Gold in these samples occurs in a number of forms.

(**i**) Small (up to 10 μm) inclusions, oval in shape, of Au-Ag-tellurides, mostly petzite (Ag_3AuTe_2), occur preferentially within chalcopyrite (Fig. 1A). Other tellurides in the ores include calaverite (crystals up to 10 μm in the matrix; e.g., Fig. 1B), altaite (PbTe, up to 50 μm, in the matrix), and hessite (Ag_2Te, ≤ 5 μm, in the chalcopyrite weathering rims).

(**ii**) The chalcopyrite grains usually display an oxidized rim, which contains gold. Based on 153 point analyses, these rims consist of Fe (average 17 wt%) – Cu (average 21 wt%) oxides with inhomogeneous composition (Figs. 1B, E, F, H); these rims also contain varying amounts of Pb (up to 21 wt%; average 6.2 wt%), Te (up to 60 wt%; average 18.9 wt%), S (average 0.7 wt%), Au and Ag. One source of Au and Ag together with minor Te are Au-Ag-

telluride inclusions, which do not survive the chalcopyrite oxidation (Fig. 1B). Within the oxide rims, Au is found as porous grains and micro- to nano-particles (Figs. 1B,E,F,H), and silver as electrum and as hessite inclusions. Elemental mapping reveals the co-location of Fe and Te in this sample, but overall there is no significant correlation amongst Te and Fe. A good correlation (R^2 = 0.93) exists between Te and Pb in the oxidized chalcopyrite rims, with Te = 4.1 times Pb on an atomic ratio basis. This could indicate the presence of submicroscopic inclusions of one or more Pb-Te phases, although no known tellurite or tellurate has a stoichiometric Te:Pb ratio > 2.

(**iii**) Grains of Au-Ag alloy up to 100 μm in size also occur in the sulfide-rich bands (Fig. 1A), and show a narrow composition range with an average Ag/(Ag+Au) of 0.114(4) (molar ratio, based on 43 point analyses). These gold grains often contain numerous quartz inclusions (Fig. 1D).

(**iv**) Microporous gold, forming xenomorphic grains up to ~500 μm in size (Fig. 1A,C,D). EMP analyses conducted with a 5 μm defocused beam (186 points) reveal that this gold is compositionally inhomogeneous, containing varying amounts of Pb (min, max, average in wt%: 0.5, 20.3, 7.2), Fe (<0.05, 22.3, 4.1), Cu (<0.05, 14.0, 5.1), Ag (0.6, 6.9, 2.0), and Te (<0.05, 32, 13).

Comparison of experimental and natural textures of microporous gold

Grains of the microporous gold from Aginskoe consist of aggregates of small fibers. The diameter of these fibers can vary within single grains, with coarse fibers having diameters ≥ 300 nm, while fine fibers have diameters ≤30 nm (Fig. 2B,C). The fibers may be longer than 5 μm in length (Fig. 2C). The fibers are aligned in consistent domains, sometime radiating, and in some cases appearing to grow perpendicular to the surface of lozenge-shaped subgrains within the porous gold grain (Fig. 2A). Imaging FIB-cut sections reveals that some of the pores (up to 75 nm in diameter) are filled with a tellurium oxide (most

131 probably tellurite), while others remain open (Fig. 2B, inset). No remnants of the parent Au
132 telluride were found within any of the imaged microporous gold grains.
133
134 The textures obtained by dealloying of calaverite grains under acidic conditions are
135 compared to those of microporous gold from Aginskoe in Figure 2. Figure 2D shows the
136 surface of a partially replaced calaverite grain; a break reveals that the gold fibers grow
137 perpendicular to the calaverite surface, resulting in radiating aggregates (see e.g. Zhao et al.
138 2009). FIB cuts through the grains show that the gold fibers (Fig. 2E,F) have diameters
139 ranging from ~60 to 250 nm.
140
141 **Discussion**

142 *Formation of microporous gold at Aginskoe*
143 The composition of microporous gold (Fig. 3) clearly reflects its formation via the
144 dealloying of a Au-(Ag) telluride (Petersen et al. 1999; Li and Makovicky 2001). The
145 transformation was complete in the investigated samples from the open cut, with no
146 remnant of the original telluride found. Calaverite is a likely precursor (Fig. 3). According to
147 Andreeva et al. (2013), calaverite is the main Au-telluride at Aginskoe, and often displays
148 partial alteration to porous gold. The Pb contents of microporous gold are due to the
149 weathering of altaite inclusions that were associated with the precursor calaverite. In the
150 investigated samples, small idiomorphic calaverite inclusions (<10 μm) are found dispersed
151 in the matrix, sometimes close to microporous gold (e.g., Fig. 1C). These relicts may have
152 been preserved in the absence of pathway for the oxidizing fluid responsible for the
153 dealloying.
154
155 During the oxidative dealloying of a gold telluride, Te is liberated into solution, probably as
156 a tellurite complex (Zhao et al. 2009). Assuming that all Te re-precipitates immediately as

This is a preprint, the final version is subject to change, of the American Mineralogist (MSA)
Cite as Authors (Year) Title. American Mineralogist, in press.
(DOI will not work until issue is live.) DOI: http://dx.doi.org/10.2138/am.2014.4792

TeO_2(s), the reaction is associated with a large volume increase in the mineral products relative to that of the reactant, e.g.,

calaverite [$AuTe_2$] + 2 O_2(aq) = gold + 2 tellurite [TeO_2] (1)

48.6 cm^3/mole 10.2 cm^3/mole 2 x 27.4 cm^3/mole; ΔV = +33.7%.

In the case of the oxidation of chalcopyrite, little sulfur remains among the products (80% of the EMP points show ≤1 wt% S), and a simplified model reaction suggests a volume deficiency:

chalcopyrite [$CuFeS_2$] + 2.5 H_2O + 4.25 O_2(aq) = goethite [FeO(OH)] + tenorite [CuO] + 2 SO_4^{2-} + $4H^+$ (2)

43.9 cm^3/mole 21.3 cm^3/mole 12.2 cm^3/mole; ΔV = -24%

Therefore, the volume loss during chalcopyrite oxidation can provide the extra space required for deposition of solid calaverite oxidation products. This coupling between the weathering of chalcopyrite and the dealloying of the telluride precursor of the porous gold accounts for the conspicuous Te contents found in the chalcopyrite alteration rims (average ~19 wt%). Only a small amount of this Te can be attributed to the destruction of petzite inclusions contained in chalcopyrite upon weathering (Fig. 1B), because of the small volumes of these inclusions. Therefore, the excess Te liberated during the dealloying (most likely as a tellurite ion) was scavenged by the chalcopyrite weathering crusts, either via sorption by Fe oxi-hydroxides, or by the formation of insoluble tellurite minerals (Grundler et al. 2013).

Zhao et al. (2009, 2010) have shown that availability of a suitable oxidant is a key control on the progress and kinetics of the oxidative dealloying of calaverite. The timing of this oxidation event is unknown at Aginskoe. The two most likely periods of influx of oxidizing waters are 1) during the late stage of mineralization, and 2) during late weathering. Chemical weathering in Kamchatka is expected to be slow, due to cold climatic conditions.

The whole of Kamchatka was underneath a glacier in the Middle Pleistocene, and Aginskoe was covered by glaciers during the last glacial maximal (~21 ky) as well (Barr and Solomina, 2013). In contrast, because epithermal systems are shallow depositional systems, influx of highly oxidizing waters during mineralization is common; for example, Mn^{4+} minerals such as cryptomelane ($K(Mn^{4+}{}_7Mn^{3+})O_{16}$) are intimately associated with high-grade ores at the ~4.5 My old Asachinskoe deposit (Takahashi et al. 2007); Asachinskoe and Aginskoe are currently the only producing Au-Ag mines in Kamchatka. These influxes of oxidizing waters may be contemporaneous with mineralization, or related to later hydrothermal circulation; such circulation is likely to occur since volcanic and associated geothermal activity are still ongoing in Kamchatka; for example, the large Pleistocene-Holocene Ichinsky stratovolcano (3621 m altitude) is less than 30 km away from Aginskoe. Chemical weathering of the ores under conditions of elevated temperatures can explain the extent of the dealloying and the absence of preservation of the precursor telluride, since under mild conditions (150-220 ˚C), experiments show very fast (over days) replacements of a variety of telluride minerals (Zhao et al. 2009, 2010, 2013; Xu et al. 2013).

Note that Te mobility in the studied samples was extensive, but occurred only over a small length scale. This length scale was limited by the coupling between the dealloying reaction and chalcopyrite weathering. Oxidized Te species are extremely fine grained (<<5 μm) and cryptic. Such occurrence may explain the lack of reported secondary Te minerals in many telluride ores found in volcanogenic and strong weathering environments, with only exceptional circumstances leading to the development of rich assemblages of secondary Te(IV) and Te(VI) minerals in the oxidation zone (Grundler et al. 2008).

Textural homology among natural and synthetic products

The textures of microporous gold from Aginskoe and those produced by the dealloying of calaverite under hydrothermal acidic conditions are remarkably similar, both in terms of morphology and size of the gold nanocrystals (Fig. 2). Xia et al. (2009) illustrated the effect of pH on the texture of the products of interface-coupled dissolution-reprecipitation reactions using the replacement of leucite ($KAlSi_2O_6$) by analcime ($NaAlSi_2O_6.H_2O$) as an example. We tested such an effect of the replacement of calaverite by gold by performing a set of experiments at high pH ($pH_{21.3\ ^oC}$ = 9.83, using a H_3BO_3/NaOH buffer). Figure 4 shows that the resulting textures indeed differ from the textures obtained under acidic condition: the gold crystallites do not display fibrous growth, but rather form a three-dimensional network of 300–1000-nm-sized crystals. The similarity in the textures of microporous gold from Aginskoe with those obtained via the oxidative dealloying of calaverite at 200 ˚C may reflect similar conditions of formation; in particular, we observed that mustard gold formed during weathering of the Au-tellurides at the Kalgoorlie gold mine is coarser than that obtained during hydrothermal synthesis. However, a better understanding of the controls on the texture of the gold obtained via such a route is required in order to gain confidence in this interpretation.

Acknowledgement

We acknowledge AINSE for funding the study conducted at ANSTO under award ALNGRA 12016; financial support from the Australian Research Council DP1095069, and financial support from the Russian Ministry of Science and Education (Programme of the Strategical Development Vitus Bering Kamchatka State University 2012-2016). We would like to thank the editor and reviewers for their helpful comments.

References

Andreeva, E.D., Matsueda, H., Okrugin, V.M., Takahashi, R., and Ono, S. (2013) Au-Ag-Te mineralization of the low-sulfidation epithermal Aginskoe deposit, Central Kamchatka, Russia. Resource Geology, 63, 337-349.

Barr, I.D., and Solomina, O. (2013) Pleistocene and Holocene glacier fluctuations upon the Kamchatka Peninsula. Global and Planetary Change. DOI:10.1016/j.gloplacha.2013.08.005

Bowell, R.J. (1992) Supergene gold mineralogy at Ashanti, Ghana: Implications for the supergene behaviour of gold. Mineralogical Magazine, 56, 545-560.

Deschênes, G., Pratt, A., Fulton, M., and Guo, H. (2006) Kinetics and mechanism of leaching synthetic calaverite in cyanide solutions. Minerals and Metallurgical Processing, 23, 133-138.

Grundler, P., Brugger, J., Meisser, N., Ansermet, S., Borg, S., Etschmann, B., Testemale, D., and Bolin, T. (2008) Xocolatlite, $Ca_2Mn^{4+}{}_2Te_2O_{12}{\cdot}H_2O$, a new tellurate related to kuranakhite: description and measurement of Te oxidation state by XANES spectroscopy. American Mineralogist, 93, 1911-1920.

Grundler, P., Brugger, J., Etschmann, B., Helm, L., Liu, W., Spry, P.G., Tian, Y., Testemale, D., and Pring, A. (2013) Speciation of aqueous tellurium(IV) in hydrothermal solutions and vapors, and the role of oxidized tellurium species in Te transport and gold deposition. Geochimica et Cosmochimica Acta, 120, 298–325.

Li, J.L., and Makovicky, E. (2001) New studies on mustard gold from the Dongping Mines, Hebei Province, China: The tellurian, plumbian, manganoan and mixed varieties: Neues Jahrbuch Fur Mineralogie-Abhandlungen, 176, 269-297.

Nie, F. J. (1998) Geology and origin of the Dongping alkalic-type gold deposit, Northern Hebei province, People's Republic of China. Resource Geology, 48, 139-158.

Petersen, S.B., Makovicky, E., Li, J.L., and Rose-Hansen, J. (1999) Mustard gold from the Dongping Au-Te deposit, Hebei Province, People's Republic of China. Neues Jahrbuch für Mineralogie-Monatshefte, 8, 337-357.

Song, G. R., Liuang, H. F., and Tian, S. (1996) Geology of Dongping Alkaline Complex-Hosted Gold Deposit in Hebei Province. - Publ. House Earthquake, pp. 181. (in Chinese, Engl. abstract, 171-174).

Takahashi, R., Matsueda, H., Okrugin, V.M., and Ono, S. (2007) Epithermal gold-silver mineralization of the Asachinskoe deposit in south Kamchatka, Russia. Resource Geology, 57, 354-373.

Takahashi, R., Matsueda, H., Okrugin, V.M., Shikazono, N., Ono, S., Imai, A., Andreeva, E.D., and Watanabe, K. (2013) Ore-forming Ages and Sulfur Isotope Study of Hydrothermal Deposits in Kamchatka, Russia. Resource Geology, v. 63, p. 210-223.

Wilson, A. F. (1984) Origin of quartz-free gold nuggets and supergene gold found in soils and laterites -a review and some new observations. Australian Journal of Earth Sciences, 31, 303-316.

Xia, F., Brugger, J., and Pring, A. (2009) Three dimensional ordered arrays of zeolite nanocrystals with uniform size and orientation by a pseudomorphic coupled dissolution-reprecipitation replacement route. Crystal Growth & Design, 9, 4902-4906.

Xu, W., Zhao, J., Brugger, J., Chen, G., and Pring, A. (2013) Mechanism of mineral transformations in krennerite, Au_3AgTe_8, under hydrothermal conditions. American Mineralogist, 98, 2086-2095.

Zhao, J., Brugger, J., Grundler, P.V., Xia, F., Chen, G., and Pring, A. (2009) Mechanism and kinetics of a mineral transformation under hydrothermal conditions: Calaverite to metallic gold. American Mineralogist, 94, 1541-1555.

Zhao, J., Xia, F., Pring, A., Brugger, J., Grundler, P.V., and Chen, G. (2010) A novel pre-treatment of calaverite by hydrothermal mineral replacement reactions. Minerals Engineering, 23, 451-453.

Zhao, J., Brugger, J., Xia, F., Nogthai, Y., Chen, G., and Pring, A. (2013) Dissolution-reprecipitation vs. solid state diffusion: Mechanism of mineral transformations in sylvanite, $(AuAg)_2Te_4$, under hydrothermal conditions. American Mineralogist, 98, 19–32, 2013.

This is a preprint, the final version is subject to change, of the American Mineralogist (MSA)
Cite as Authors (Year) Title. American Mineralogist, in press.
(DOI will not work until issue is live.) DOI: http://dx.doi.org/10.2138/am.2014.4792

Figures captions

Figure 1. Modes of occurrence of gold at the Aginskoe gold deposit. **A.** Overview of high grade band. **B.** Chalcopyrite grain with oxidized rim. Gold is present as oval inclusion of Au-Ag tellurides (mainly petzite) within the chalcopyrite. **C.** Overview of a microporous gold grain from Aginskoe. **D.** Grains of Au-Ag alloy with many quartz inclusions in contact with microporous gold and Fe-oxy-hydroxides. **E.** Detail of oxidation rim around chalcopyrite. **F.** High-resolution image showing the redistribution of Au in the rim in the form of micro- to nano-particles. **G.** Location of FIB cut. **H.** RGB image (red – Au; green – Cu; blue – Fe) of the FIB cut and surrounding area, showing inhomogeneous distribution of Cu and Fe, and the presence Au particles. Te is associated with Fe in this area. Abbreviations: Au, native gold; p-Au, microporous native gold; cal, calaverite; cpy, chalcopyrite; o-cpy, oxidized chalcopyrite; ptz, petzite; Te-O, Te-rich oxide minerals. A-F SEM BSE images, G SE-SEM, and H X-ray image.

Figure 2. Comparison of the microtextures of porous gold from the Aginskoe deposit (**A-C**) with those of synthetic Au (and Au-Ag alloy) obtained experimentally via the de-alloying of calaverite at 200 ˚C and $pH_{24.6C}$ = 1.86 (**D-F**). Horizontal stripes in **E** are due to charging on the uncoated, freshly cut surface.

Figure 3. Triangular plot showing the Au, Ag and Te contents of porous and non-porous gold, oxidized chalcopyrite rims (o-cpy), and the tellurides calaverite, hessite and petzite in the investigated samples from Aginskoe.

Figure 4. Effect of pH on the porous gold textures obtained via replacement of calaverite. Textures in this figure were obtained at $pH_{21.3\ ^oC}$ = 9.83; compare with textures obtained at $pH_{24.6\ ^oC}$ = 1.86 in Fig. 2D,E,F.

This is a preprint, the final version is subject to change, of the American Mineralogist (MSA)
Cite as Authors (Year) Title. American Mineralogist, in press.
(DOI will not work until issue is live.) DOI: http://dx.doi.org/10.2138/am.2014.4792

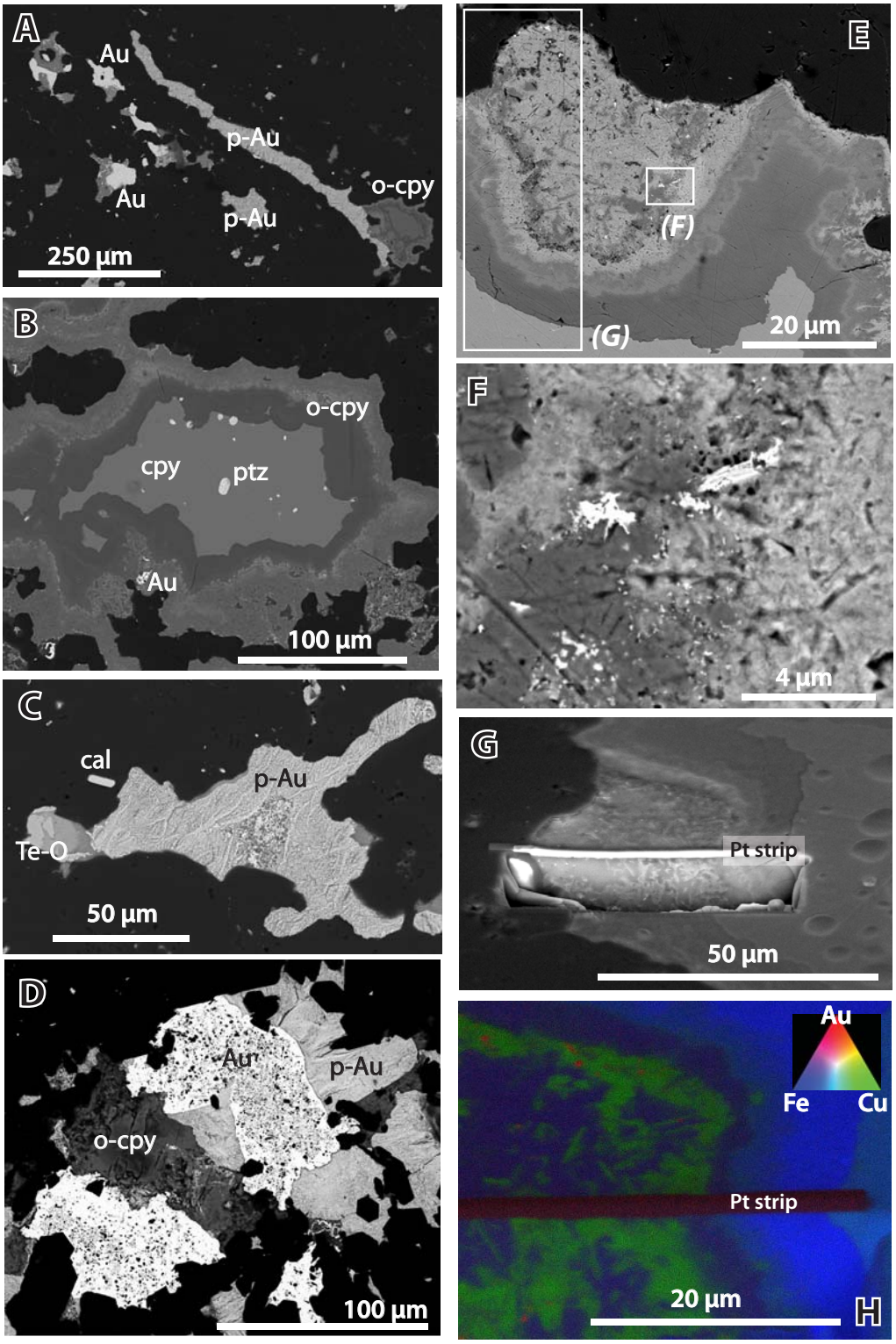

This is a preprint, the final version is subject to change, of the American Mineralogist (MSA)
Cite as Authors (Year) Title. American Mineralogist, in press.
(DOI will not work until issue is live.) DOI: http://dx.doi.org/10.2138/am.2014.4792

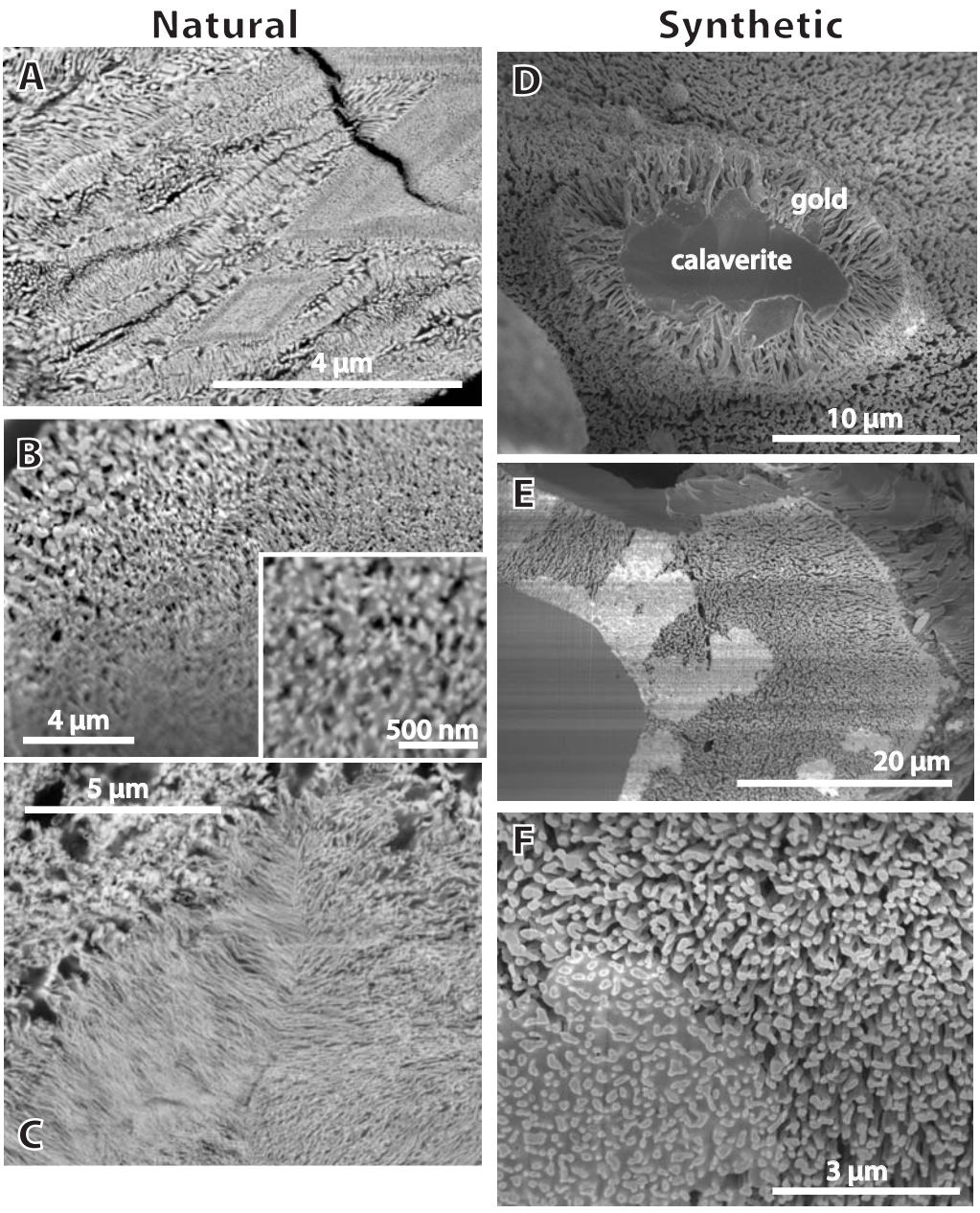

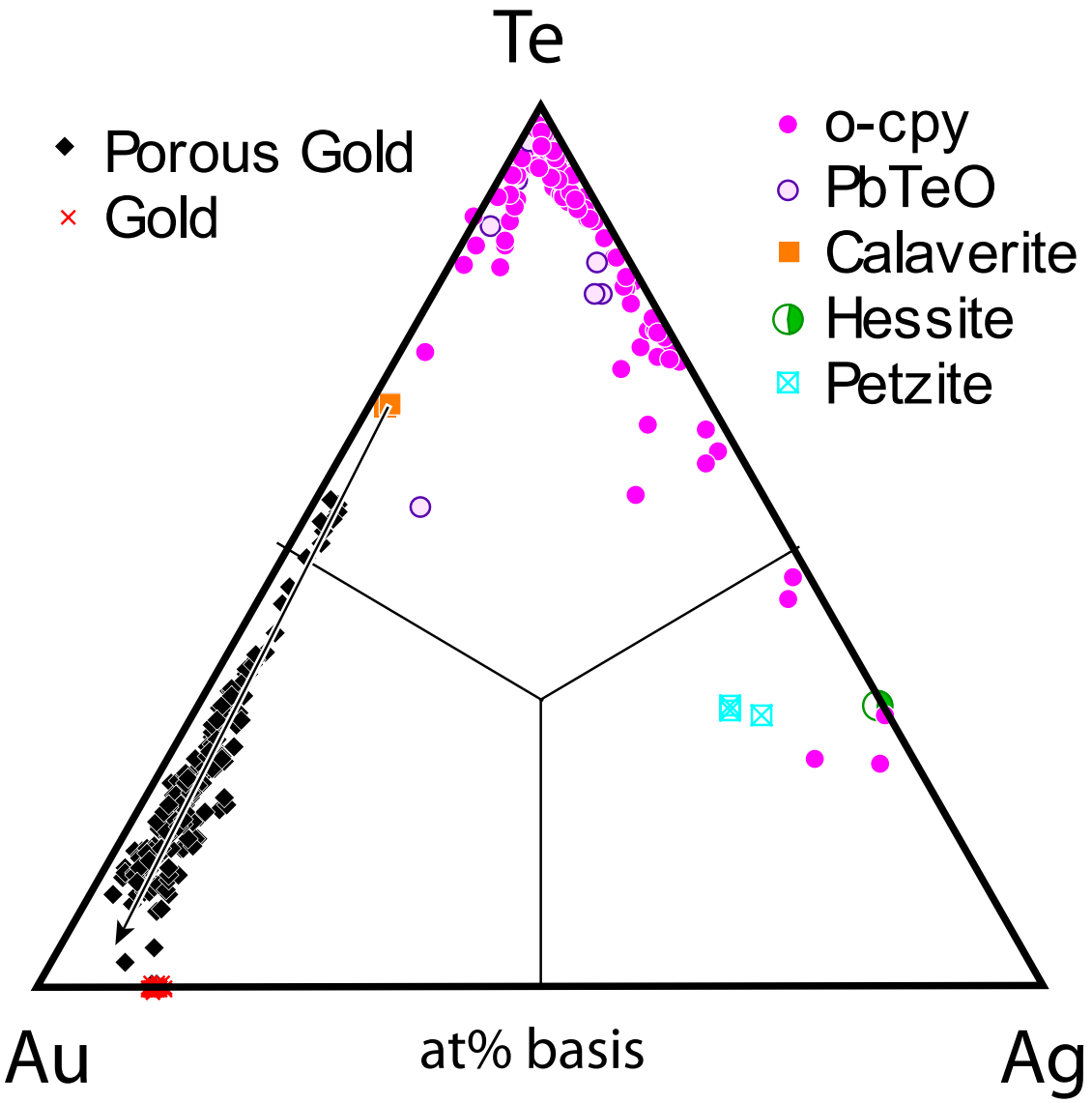
Te
Porous Gold
Gold
o-cpy
PbTeO
Calaverite
Hessite
Petzite
Au
at% basis
Ag

This is a preprint, the final version is subject to change, of the American Mineralogist (MSA)
Cite as Authors (Year) Title. American Mineralogist, in press.
(DOI will not work until issue is live.) DOI: http://dx.doi.org/10.2138/am.2014.4792